Joint International Topical Meeting on Mathematics & Computation and Supercomputing in Nuclear Applications (M&C + SNA 2007)
Monterey, California, April 15-19, 2007, on CD-ROM, American Nuclear Society, LaGrange Park, IL (2007)

DEGRADATION MONITORING IN IRIS STEAM GENERATORS

Bulent Alpay, James Paul Holloway and John C. Lee
Department of Nuclear Engineering and Radiological Sciences
University of Michigan
Ann Arbor, MI 48109
balpay@umich.edu; hagar@umich.edu; jcl@umich.edu

ABSTRACT

We present a degradation monitoring technique based on unscented Kalman filtering (UKF), which uses a nonlinear system model without linearization to estimate the status of the component/state variables. To test the applicability of the methodology, the fouling of tubes is chosen among various degradation mechanisms for the IRIS (International Reactor Innovative and Secure) steam generators (SGs). The degradation monitoring algorithm diagnoses the tube fouling and estimates the thickness of the crud deposited on the secondary side of the SG along with the increase in the pressure drop triggered by fouling. A stand-alone SG model developed with the RELAP5 code was used to simulate the transient behavior of the SG and drive an UKF state estimate. By using the secondary side outlet temperature as the measurement and the nodal pressures along the secondary side as states, UKF generated accurate estimates of the crud layer thicknesses for different crud formations.

Key Words: Degradation Monitoring, Unscented Kalman Filtering, IRIS Steam Generator.

1. INTRODUCTION

For the next generation of nuclear power plants (NPPs), it is crucial to monitor, diagnose and predict component degradations to ensure both increased safety and improved economics. Since steam generators (SGs) are one of the most vulnerable parts of a NPP, online degradation monitoring will help to maintain a high level of safety and performance in the plant. This would especially be the case in IRIS (International Reactor Innovative and Secure), where all the primary system components including pumps, steam generators, pressurizer, and control rod drive mechanisms, are located inside the reactor vessel.

The model-based degradation monitoring technique we used is based upon component/state estimation. This approach assumes that degradations in component states will cause changes to certain system states and measurements. By monitoring the estimated system states, it is then possible to detect and isolate each fault. With this approach, it is essential to have a computational model to connect the system state to the component state, so that changes in component state can be seen through their symptoms as changes in plant behavior.

For nonlinear Gaussian dynamic state space models, in our earlier study [1] we used the extended Kalman filter (EKF) approximation, which is valid if all the higher order derivatives of the nonlinear functions are negligible over the monitored region of state variables. This has large implications for the accuracy and consistency of the resulting EKF algorithm. These

approximations often introduce large errors in the EKF calculated posterior mean and covariance of the transformed Gaussian random variable (GRV), which may lead to suboptimal performance and sometimes divergence of the filter.

The unscented Kalman filter (UKF) has been proposed in an attempt to address these issues. It is a derivativeless, deterministic sampling based on the Kalman filter structure and consistently outperforms the EKF not only in terms of estimation accuracy, but also in filter robustness and ease of implementation [2].

2. UNSCENTED KALMAN FILTERING

The UKF is a recursive minimum mean square error estimator in the framework of the Kalman filter that addresses some of the approximation issues of the EKF. Unlike the EKF, the UKF does not approximate the nonlinear process and observation models; it uses the complete nonlinear models and rather approximates the distribution of the state random variable. In the UKF the state distribution is still represented by a GRV, but it is specified using a minimal set of deterministically chosen sample points. These sample points completely capture the true mean and covariance of the GRV, and when propagated through the true nonlinear system, capture the posterior mean and covariance accurately to the second order for any nonlinearity, with errors only introduced in the third and higher orders [2].

Consider the discrete-time nonlinear dynamic system with joint state $z = [x \;\; c]^T$ where x and c are system and component state variables, respectively, with process noise w. Also let the measurement y by subject to noise ν, so that the system and measurement are modeled by

$$z(k) = f[z(k-1), w(k-1)], \qquad \left\langle w(k-1), w^T(k-1) \right\rangle = Q(k-1), \tag{1}$$

$$y(k) = h[z(k), \nu(k)], \qquad \left\langle \nu(k) \nu^T(k) \right\rangle = R(k). \tag{2}$$

Given mean $\hat{z}$ and covariance P_{zz} for $z(k-1)$, to calculate the statistics of the measurement a set of $2L+1$ sigma points χ_i, with associated weights ω_i and scaling parameter γ, are chosen

$$\{\chi_i\} = \left\{ \hat{z} \qquad \hat{z} + \left(\gamma \sqrt{P_{zz}}\right)_i \qquad \hat{z} - \left(\gamma \sqrt{P_{zz}}\right)_i, \quad i = 1, \ldots, L \right\}, \tag{3}$$

so that they completely capture the true mean and covariance of the joint state z. With the transformation of sigma points,

$$\chi_i(k) = f[\chi_i(k-1)], \qquad Y_i(k) = h[\chi_i(k)], \tag{4}$$

we can reconstruct the posterior statistics from the propagated sigma points using a weighted sample mean and covariance

$$\hat{z}^-(k) = \sum_{i=0}^{2L} \omega_i \chi_i(k), \qquad \hat{y}(k) = \sum_{i=0}^{2L} \omega_i Y_i(k), \tag{5}$$

$$P_{zz}^-(k) = \sum_{i=0}^{2L} \omega_i [\chi_i(k) - \hat{z}^-(k)][\chi_i(k) - \hat{z}^-(k)]^T + Q(k), \tag{6}$$

$$P_{zy}(k) = \sum_{i=0}^{2L} \omega_i [\chi_i(k) - \hat{z}^-(k)][Y_i(k) - \hat{y}(k)]^T, \quad (7)$$

$$P_{yy}(k) = \sum_{i=0}^{2L} \omega_i [Y_i(k) - \hat{y}(k)][Y_i(k) - \hat{y}(k)]^T + R(k). \quad (8)$$

The optimal system estimate following the measurement $y(k)$ is obtained in a standard Kalman filter structure as

$$\hat{z}(k) = \hat{z}^-(k) + K(k)[y(k) - \hat{y}(k)], \quad (9)$$

with the Kalman gain

$$K(k) = P_{zy}(k) P_{yy}^{-1}(k), \quad (10)$$

and the state covariance is updated

$$P_{zz}(k) = P_{zz}^-(k) - K(k) P_{xy}^T(k). \quad (11)$$

3. APPLICATION TO IRIS SG MODEL

There are various degradation mechanisms for SGs including stress corrosion cracking, denting, pitting, fretting, wear, and fouling. Once an algorithm for online degradation monitoring is constructed, it can be applied to all types of SG degradation mechanisms if there is a model for the degradation. We started testing our algorithm with SG fouling.

3.1. SG Fouling

Fouling is defined as the formation on heat transfer surfaces of undesired deposits, which impede the heat transfer and increase the resistance to fluid flow, resulting in higher pressure drop. The growth of the deposits causes the thermo-hydraulic performance of the SG to degrade with time. In environments such as SGs where the heat flux is high, fouling can lead to local hot spots and it may result in mechanical failure of the heat transfer surface [3]. The progression of fouling with time and its effect on thermal performance are shown in Fig. 1.

3.2. IRIS SG

The IRIS SG is a helical-coil once-through design with the primary fluid flowing outside the tubes. Eight SG modules are located in an annular space between the core barrel and reactor vessel. Feedwater enters the SG through a nozzle in the reactor vessel wall and passes through the lower feed water header. The feedwater enters the SG tubing, and is heated to saturation, boiled to steam, and superheated as it flows upward to the upper steam header [4].

In our earlier study [5], we utilized a simplified one dimensional movable boundary formulation for the modeling of fouling in IRIS SG in which we only studied the effect on the heat transfer characteristics. In this work, we adopted a stand-alone IRIS SG model for the RELAP5 code [6] to simulate a tube fouling scenario and test the applicability of our online degradation monitoring

algorithm. The stand-alone SG model was constructed by using the RELAP5 model developed by Westinghouse, Polytechnic of Milan and University of Zagreb [7]. We used the same nodalization for the primary and secondary sides of the SG by using the nominal conditions of the SG primary and secondary side inlets as boundary conditions

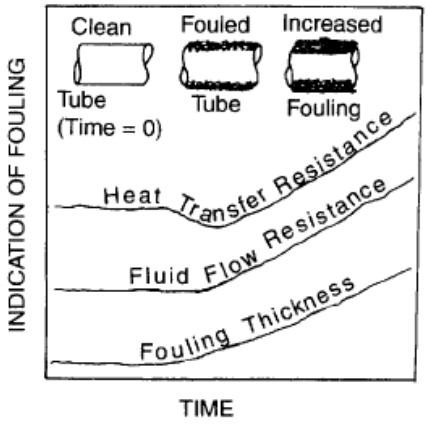

Figure 1. The progression of fouling with time [3].

3.3. Modeling of Fouling in RELAP5

RELAP5 doesn't contain the necessary routines to practice SG fouling applications. We wrote a Python [8] script to add a crud layer gradually into the RELAP5 model. The script needs the deposition rate and location as inputs and generates the input for RELAP5 which is run for a time interval where the crud deposition is assumed to be constant. Then the script processes the output of RELAP5 to prepare the input for the next time interval. This loop is terminated when the crud layer no longer changes.

We assumed that crud formation occurs at 10 s after the start of the simulation, rather than a slow deposition over years of operation. We simulated the fouling of the SG tubes by considering crud buildup uniformly inside the SG tubes.

3.4. UKF Implementation

We chose UKF for not only being a better approximation than EKF for highly nonlinear systems, but also its ease of applicability especially when the model is represented by pre-compiled computer codes like RELAP5 in which calculation of Jacobians can be very time consuming and difficult.

In our implementation, the plant behavior is observed through the temperature at the outlet of the secondary side. The system states are represented through the pressure distribution inside the secondary side tubes and pressure drop is calculated through these states. The component state to be estimated is the crud layer thickness.

The SG tubes in IRIS are assumed to be composed of Inconel Alloy 690. Since the formation and thickness of the crud is not known, we tried our algorithm for different values of thermal conductivity and different thicknesses of the crud. We started our analysis by assuming the thermal conductivity of the crud layer is ~50% less than the thermal conductivity of Inconel Alloy 690 in the operating temperature range. We introduced a 0.5 mm crud layer deposition along the length of the tubes and simulated the measurement, which is the temperature at the outlet of the secondary side with 0.5% noise added. The simulated measurement, and the estimated measurement (through UKF as a state) obtained through Eq. (5) is shown in Fig. 2.

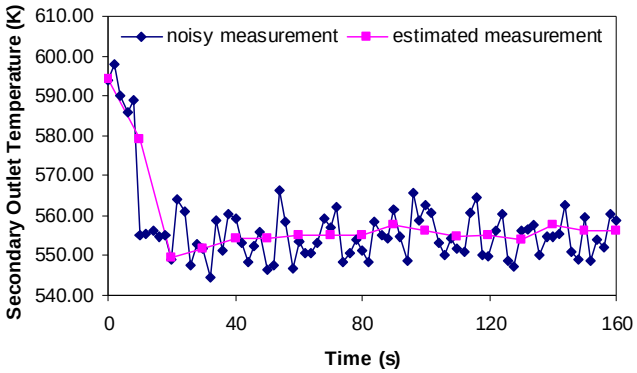

Figure 2. Simulated and estimated measurement for 0.5 mm crud thickness and 50% decrease in thermal conductivity of Inconel.

We applied the UKF to obtain a best estimate of the thickness of the crud layer, considered as a component state [Fig. 3(a)], together with a best estimate of the pressure drop along the secondary side [Fig. 3(b)].

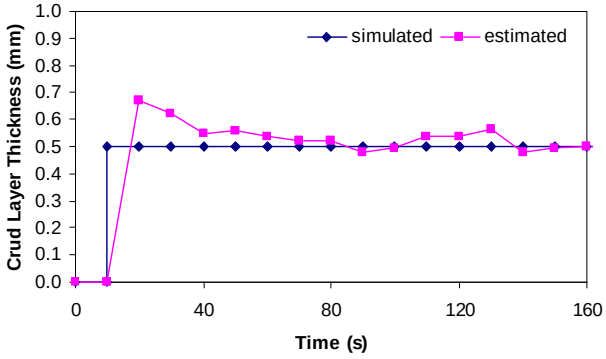

(a) Crud layer thickness

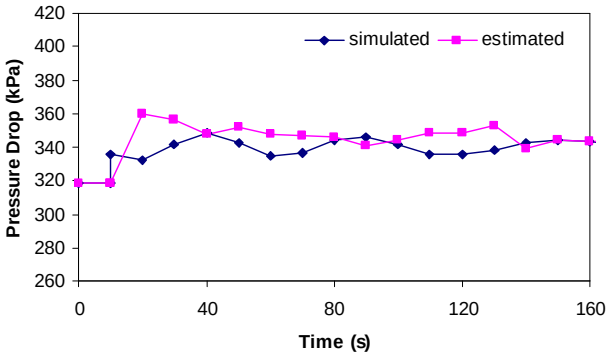

(b) Secondary side pressure drop

Figure 3. Simulated and estimated component and system states for 0.5 mm crud thickness and 50% decrease in thermal conductivity of Inconel.

Even though it is unrealistic, it is harder to estimate the thicknesses of the crud layers which have thermal conductivities close to the Inconel tubes. Therefore, in a second case, we assumed the thermal conductivity of the crud layer is ~25% less than the thermal conductivity of Inconel Alloy 690 in the operating temperature range. In order to test this problem, we introduced three different crud layer deposits along the length of the tubes as 0.25 mm, 0.5 mm and 1 mm, and then we simulated the real plant behavior by adding white Gaussian noise through RELAP5. The thicknesses of the crud layers and the pressure drop along the secondary side were estimated through UKF and the corresponding estimation errors were obtained as shown in Fig. 4.

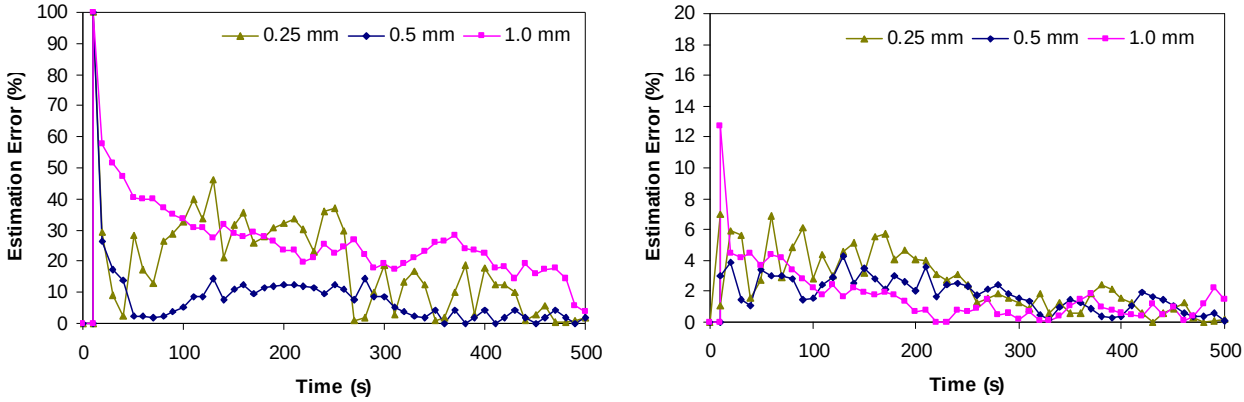

(a) Crud layer thickness (b) Secondary side pressure drop

Figure 4. Estimation errors for 25% decrease in thermal conductivity of Inconel.

For both cases, UKF algorithm successfully diagnosed and estimated the change in crud layer thicknesses and the change in the pressure distributions inside the SG tubes by which we calculated the change in the secondary side pressure drops.

This technique is sensitive to both material properties and thicknesses of the crud in terms of the time for convergence. By introducing three different crud layer thicknesses as 0.25 mm, 0.5 mm and 1.0 mm, and three different crud thermal conductivities, which were set to 25%, 50% and 75% less than the thermal conductivity of the SG tubes, we ran UKF and calculated the estimation errors at 160 s as given in Fig. 5.

Although UKF results eventually converge to the true component/system states, for the estimation of the crud layer thickness it takes a longer time to converge if the thermal conductivity of the crud is close to thermal conductivity of Inconel or if a large layer of crud is introduced abruptly. For estimation of the pressure drop, the convergence time increases as the thickness of the crud layer gets smaller.

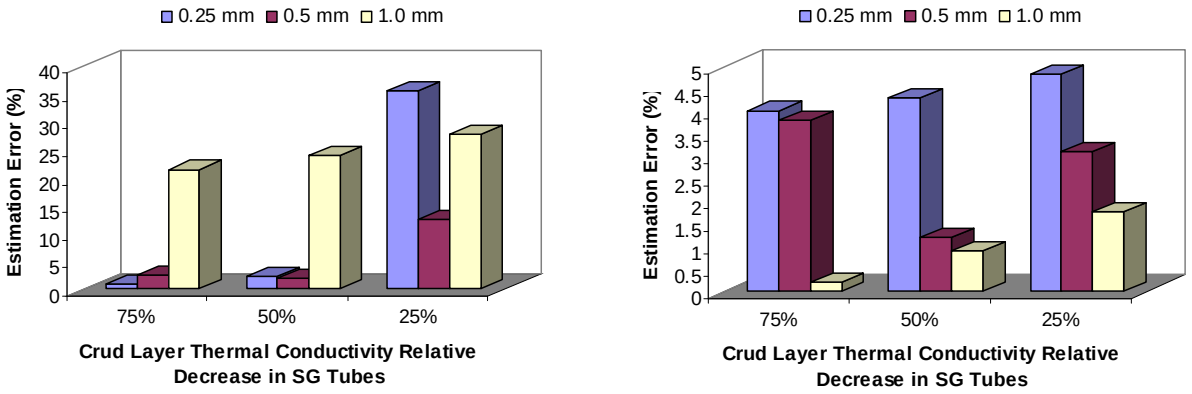

(a) Crud layer thickness

(b) Secondary side pressure drop

Figure 5. Estimation errors for various crud thicknesses and thermal conductivities at 160 seconds.

4. CONCLUSIONS

We utilized the UKF for degradation monitoring of the IRIS SG because of its estimation accuracy for highly nonlinear systems and ease of implementation when the model is represented by complex computer codes rather than by simple analytical expressions. With SG fouling chosen as the degradation mechanism, our UKF diagnostic algorithm provides accurate estimates of the crud layer thicknesses. These estimates were achieved by coupling a RELAP5 model to the UKF. The next step is to modify the model such that one can also estimate the radial and axial location of the crud layer along with its thickness to predict the lifetime of the SG tubes.

ACKNOWLEDGEMENTS

This work was supported by DOE grant DE-FG07-02SF22612.

REFERENCES

1. S. E. Aumeier, B. Alpay, J. C. Lee, and A. Z. Akcasu, “Probabilistic Techniques for Diagnosis of Multiple Component Degradations,” *Nuclear Science and Engineering*, **153**, 2, 101-123 (2006).
2. S. J. Julier, J. K. Uhlmann, “A New Extension of the Kalman Filter to Nonlinear Systems,” *Proc. SPIE - Int. Soc. Opt. Eng.* Orlando, FL, **3068**, pp. 182–193 (1997).
3. N. Zelver, F. L. Roe and W. G. Characklis, “Monitoring of fouling deposits in heat transfer tunes: Case Studies,” *Industrial Heat Exchangers Conf. Proc.*, American Society of Metals, OH (1985).
4. M. D. Carelli, et. al., “The Design and Safety Features of the IRIS Reactor,” *Proc. 11th International Conference on Nuclear Engineering, (ICONE-11)*, Tokyo, Japan, April 20-23 (2003).

5. B. Alpay, J. C. Lee, “Degradation Monitoring through Unscented Kalman Filtering,” *Trans. Am. Nucl. Soc.*, **94**, 579 (2006).
6. "RELAP5/MOD3.3 Code Manual, Volume 1: Code Structure, Systems Models, and Solution Methods," NUREG/CR-5535, Rev. 1, U. S. Nuclear Regulatory Commission (2001).
7. T. Bajs, et al., “Development of RELAP5 Nodalization for IRIS Non-Loca Transient Analyses,” *American Nuclear Society Topical Meeting in Mathematics & Computations (M&C)*, April 6-10, 2003, Gatlinburg, TN, USA (2003).
8. G. Van Rossum et al., “Python Language Website”, http://www.python.org/ (2007).